Int. J. Microgravity Sci. Appl., **35** (3) (2018) 350303
DOI: 10.15011//jasma.35.350303

IIII Original Paper IIII

Crystallization of Charged Colloids under Microgravity during Aircraft Parabolic Flights

Yuki TOMITA[1], Tomotaka SEKI[1], Nao FUKAYA[1], Suguru NISHIKAWA[1], Naoko SATO[1], Mami IMAI[1], Misato SUKO[1], Mio TAKAKI[1], Yurina AOYAMA[1], Akiko TOYOTAMA[1], Tohru OKUZONO[1], Junpei YAMANAKA[1], Katsuo TSUKAMOTO [2] and Yuko INATOMI[3]

Abstract

We studied crystallization process of charged colloids under microgravity (μG) by performing time resolved reflection spectroscopy, during aircraft parabolic flight experiments. We used dilute colloidal silica samples (specific gravity of the particles = 2.1, the particle concentration = 1 – 2 vol.%) that crystallized from shear-melt colloids, within the duration time of μG (approximately 20 seconds). An influence of μG was found to be less significant for the heterogeneous nucleation process with the aid of the cell walls. The incubation times of the homogeneous nucleation, τ, at μG was longer than that at 1G. Furthermore, the half-widths of the Bragg diffraction peaks from the crystals were narrower by 30% at the largest, under μG. This suggests that the crystal grain size (cross-sectional area) became larger under μG environment, according to the Scherrer's relation.

Keyword(s): Colloidal crystals, Crystal growth, Microgravity experiments, Parabolic flight, Reflection spectroscopy, Incubation time.
Received 7 May 2018, accepted 4 July 2018, published 31 July 2018.

1. Introduction

Colloidal systems provide models to study phase transition in general [1-5]. Previous studies have revealed that phase behavior of colloids is significantly influenced by gravity [6-11] . However, the effect of gravity on colloidal crystallization was still controversial[7-10]. Furthermore, little is known whether the gravity effect is equivalently significant for both homogeneous and heterogeneous nucleation processes. In the present paper, we report the crystallization of charged colloids under microgravity (μG). In particular, we examined an influence of the gravity on incubation time τ of nucleation.

Dispersions of submicron-sized charged colloidal particles exhibit a phase transition from disordered "fluid" state to ordered "crystal" state, upon increasing a magnitude of electrostatic interparticle interaction[1-5]. **Figure 1** shows optical micrographs of the charged colloids in (a) disordered "fluid" and (b) ordered "crystal" states (sample: an aqueous dispersion of charged polystyrene particles, diameter = 430 nm, particle concentration C_p = 1 vol.%) [12]. In the crystal states the colloidal particles are arranged regularly in the face-centered-cubic (FCC) or body-centered-cubic (BCC) lattice symmetry, while the particle positions have only short-range order in the fluid states[2-5]. The Bragg wavelength of the colloidal crystals often lay in the visible light wavelength regime. In addition, dynamics of the colloids is much slower than that in atomic and molecular systems. These characteristics of colloids enable *in-situ* examination of the crystallization process by means of conventional spectroscopy [5,7-10,13].

Colloidal particles undergo gravitational sedimentation unless the specific gravity of medium is adequately matched to that of particles. The influence of sedimentation appears to be more significant at the initial stage of the crystallization, where crystal nuclei are formed in disordered fluid. Furthermore, convection currents due to temperature inhomogeneity in the samples, if any, may affect the nucleation. Thus, short-duration μG environment attained by aircraft parabolic flights is quite useful to understand the effect of gravity on colloidal crystallization.

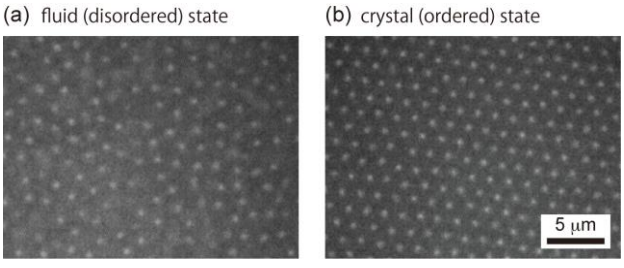

Fig. 1 Optical micrographs of (a) fluid (disordered) and (b) crystal (ordered) states of charged polystyrene colloids. Here the crystallization was controlled by temperature by using adsorption of ionic surfactant[12].

1 Nagoya City Univ., 3-1 Tanabe-dori, Mizuho-ku, Nagoya, Aichi 467-8603, Japan.
2 Osaka Univ., Toyonaka, Osaka 560-0043, Japan/Tohoku Univ., Aramaki, Aoba, Sendai 980-8578, Japan.
3 ISAS, JAXA, Sagamihara, Kanagawa 252-5210, Japan.
(E-mail: yamanaka@phar.nagoya-cu.ac.jp)

Furthermore, μG may affect the crystallization rate and crystal (or crystal grain) size (**Fig. 2**).

Thus far, colloidal crystallization under μG has been studied for hard sphere colloids[6] and also charged colloids[7-10]. A significant influence of gravity-induced stresses on the crystal shapes has been observed[6]. The dynamics of crystallizations under μG, which has been investigated for proteins in solutions [14], has not extensively studied for colloids. By performing sounding rocket experiments, Ishikawa et al. have studied the crystallization process of charged polystyrene (specific gravity (ρ) = 1.05) colloids. They reported that (i) a variation of the crystal size over time, estimated by applying time-resolved spectroscopy, obeyed a power-law, and (ii) the growth at μG was faster than that at 1G. On the other hand, Okubo et al., have reported that the crystallization rate v of charged colloidal silica (ρ = 2.1) was reduced (by about 25%) under μG by parabolic flight experiments[8,9]. They also reported that v values for silica particle in binary polystyrene/silica colloids were rather increased[15]. Shöpe et al. have reported that no significant effect of μG was observed for v of silica particle[10] at μG obtained by parabolic flight experiments. Thus the influence of μG on colloidal crystallization is still controversial.

We have performed the parabolic flight experiments in January and February 2016, in collaboration with Japan Aerospace Exploration Agency (JAXA) and Diamond Air Service (DAS) Co., Ltd, at the Nagoya airport, Aichi, Japan. We studied the crystallization of charged colloids by applying time-resolved reflection spectroscopy, which had been also employed in previous experiments[7-9,15]. We used aqueous dispersions of colloidal silica particles whose crystallization is significantly influenced by the gravity [11]. We did not observe remarkable μG effect on the crystallization rate, while incubation time of the nucleation and peak width of the reflection spectra were significantly influenced by μG.

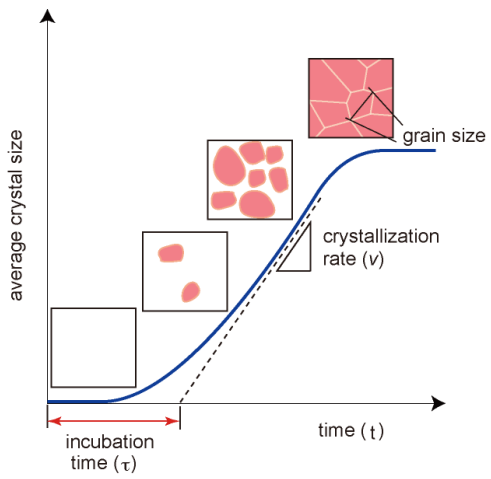

Fig. 2 Illustration of crystallization process and time evolution of crystal size.

2. Experimental Section

2.1 Materials

Aqueous dispersion of colloidal silica particles, Seahoster KE-10W, was purchased from Nippon Shokubai Co., Ltd. (Osaka, Japan). Colloidal silica Silibol 132 was kindly donated by Fuji Chemical Co., Ltd. (Osaka, Japan). They were purified by dialysis in cellulose tubes (pore size = 2.4 nm) against purified water for more than 30 days. After a mixed bed of cation- and anion-exchange resin beads (AG 501-X8 (D), Bio-Rad Labs., CA, U.S.A.) was added, the sample was kept standing for at least 1 week for further deionization. The particle diameters estimated by the dynamic light scattering method were 105 nm (KE-10W) and 132 nm (Silibol 132), respectively. The charge number Z of the purified KE-W10 particle, determined by the electrical conductivity measurements, was 170 (surface charge density σ = 0.07 μC·cm^{-2}). A 50 μM NaOH was added KE-W10 silica to increase Z for crystallization. Z of Silbol 132 was 1410 (σ = 0.41 μC·cm^{-2}).

Water was purified by using a Milli-Q system (Millipore, MA, U.S.A.) and its electrical conductivity was 0.4–0.6 μS·cm. For sample preparations, polystyrene or Teflon apparatus was used instead of glassware in order to avoid the elution of ionic impurities from the container wall. Further experimental details have been described earlier[12,13].

2.2 Methods

We have performed the parabolic flight experiments in a MU-300 jet aircraft operated by DAS Co., Ltd. The parabolic flights provided short-duration (approximately 20 seconds) μG conditions of less than 0.03 G. The μG environments were attained approximately 10 times, successively in a single flight.

The experimental setup used are illustrated in **Fig. 3(a)**. It was composed of video cameras and fiber-optics spectrophotometers (type USB2000, Ocean optics Co., Ltd., FL, U.S.A.) equipped with a Y-blanched optical fiber. Colloid samples were introduced in optically-transparent poly(methyl-methacrylate) cells (inner dimension: 1 × 1 × 2 cm). Teflon-coated magnetic bars had been put in the sample cells that were placed on magnetic stirrers. **Fig. 4(a)** and **4(b)** displays overviews of the set-up and two colloid crystal samples in the cells.

A 14 W tungsten halogen lamp was used as a light source. We used both right-angle and oblique (incident angle = 10 degree) beams, to study heterogeneous nucleation from the cell wall, and homogeneous nucleation in the bulk of the sample, as illustrated in **Fig. 3(b)**; A and B represent the crystals grown from wall by inhomogeneous nucleation and those formed inside due to homogeneous nucleation, respectively. The results will be described in Section 3.2. The reflection spectra were recorded at a time interval of 0.5 sec, and also displayed in a PC monitor during the flights.

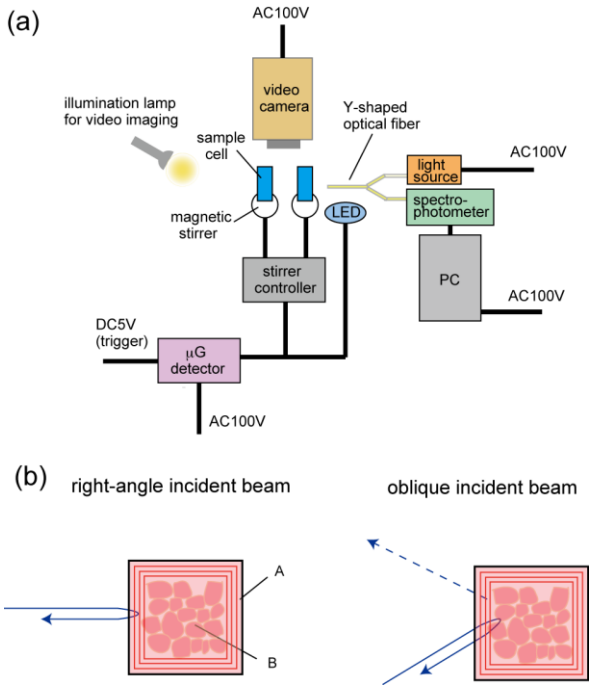

Fig. 3 (a) Setup used for the parabolic flight experiments. (b) Crystal structures and incident beam angles. A and B represent the crystals grown from wall by inhomogeneous nucleation and those formed inside due to homogeneous nucleation, respectively.

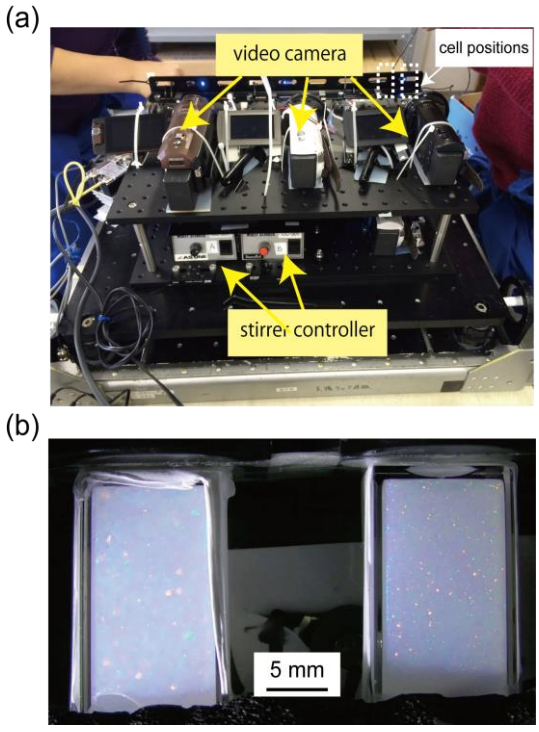

Fig. 4 (a) Overview of the experimental setup and (b) samples cells. Interference colors are originated from colloidal crystals.

The charged colloidal crystals, which are formed in liquid media by long-range electrostatic interaction, easily melt by shearing[16]. Before reaching μG, colloid samples had been kept stirring by means of the magnetic stirrer in order to maintain the samples in melt (fluid) states. Recrystallization processes from the shear-melt states were examined under μG, by stopping the stirring. To initiate the crystallization immediately after attaining the μG environments, we used a specially designed device, which had been developed by Y.I., ISAS, JAXA, for the present flight experiments. This device equipped with an electric relay circuit that disconnected the magnetic stirrers, triggered by a DC5V signal from a μG sensor of the aircraft. It also equipped with a blue LED (an emission wavelength = approximately 470 nm), which turned off when μG reached. Thus, we could record the starting time of the μG, both in the video images and reflection spectra.

Control experiments at 1G were carried out in the aircraft, before taking off and after landing, for all the flights. In the followings, we will denote these data as those before 1G and after 1G they were obtained approximately 1 hour before and 1 hour after the parabolic flight (a successive, about 10 times μG experiments), respectively.

3. Results and Discussion

3.1 Time Resolved Spectroscopy

Figure 5(a) shows a typical reflection spectra during crystallization of silica colloid under μG. Here we used KE-10W dispersion of C_p = 4 vol.%, and [NaCl] = 4 μM. Right-angle reflection spectra were recorded at a time interval of 0.5 sec after μG was attained at time t = 0 sec. A magnified spectra for the initial stage is shown in an inset figure. Video images showed that the resulted crystal was composed of small crystal grains (< 1 mm), and almost entire samples were crystallized within approximately 20 sec. A distinct peak due to Bragg diffraction appeared and its intensity increased significantly over time (**Fig. 5(b)**), after an incubation time.

Figure 5(c) represents a time variation of the peak wavelength λ_m. Distinct peak was observed at t = approximately 4 sec, and then the peak shifted to shorter wavelength. This blue shift of the Bragg peak was also observed for control experiments at 1G. A similar peak shift has been reported in previous μG experiments using polystyrene particles[7]. The broad peaks at the initial stage in **Fig. 5(a)** are presumably attributable to local, short-range ordered structures, which were formed prior to the crystal growth process. The larger wavelength observed for these local structure indicated that they had lower density that the bulk crystals.

The value of λ_m of crystalline materials is related to the lattice spacing d in the crystals by the Bragg relation $2d = n\lambda_m / n_r$ for

the right-angle diffraction; here n is an integer and n_r the averaged refractive index of the sample. For dilute aqueous silica colloids, we can safely assume that $n_r = (1\text{-}\phi)\, n_{r,w} + \phi\, n_{r,s}$, where $n_{r,w}$ and $n_{r,s}$ are refractive indexes of water (1.33) and silica particles (1.45), respectively. When the crystals are homogeneous and volume-filling, diffractions from the BCC (110) and FCC (111) lattice planes [5, 6] respectively give

$$\lambda_m = \sqrt{2}\, n_r\, (8\pi/3\phi)^{1/3} a_p \quad (1)$$

and,

$$\lambda_m = (2/\sqrt{3})\, n_r\, (16\pi/3\phi)^{1/3} a_p \quad (2)$$

Here a_p is the particle radius and ϕ the particle volume fraction. At C_p = 4vol% (ϕ = 0.04), we have λ_m = 589 nm and 683 nm for the BCC and FCC lattices. The observed value of λ_m at t > 10 sec was approximately 588 nm, which shows a close agreement with the calculated value for the BCC lattices.

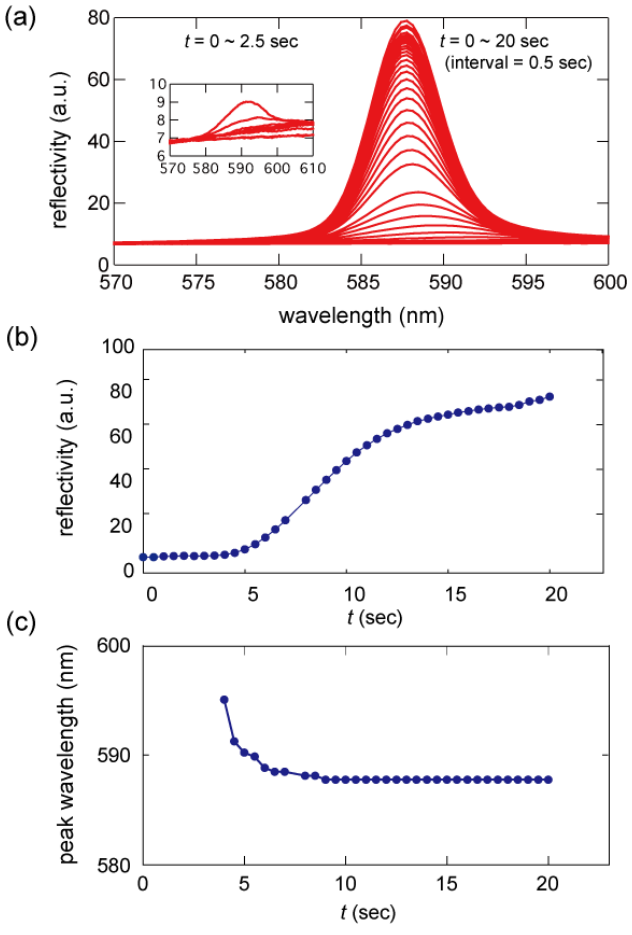

Fig. 5 (a) Variation of the reflection spectra (KE-W10, C_p = 4 vol.%;[NaCl] = 4 μM; [NaOH] = 50 μM, Right-angle incidence). Time t = 0 –25 sec; taken with an interval of 0.5 sec. An inset figure shows magnified spectra for 0–2.5 sec. Time evolutions of (b) the peak intensity and (c) peak wavelength are shown in and respectively.

3.2 Comparison Between the Right Angle and Oblique Diffractions

The higher order lattice planes of BCC crystal, having indexes (h k l) = (200), (211), (220) ・・・, give the diffraction at λ_m satisfying $2d_{hkl} = n\, \lambda_m/n_r$, where $d_{hkl} = a/(h^2 + k^2 + l^2)^{1/2}$ and a is the lattice constant[17]. The λ_m values of the first order (n = 1) diffractions from the BCC lattice planes have ratios of 1: √2: √3・・・. **Figure 6** compares the reflection spectra for an identical crystal sample under 1G, taken by using (a) right-angle and (b) oblique incident beams (sample: Silbol 132, C_p = 2 vol.%). The two peaks observed in the right-angle reflection spectra were attributable to the first and second order (n = 1 and n = 2) diffractions from BCC (110) crystal lattice planes, which were oriented *parallel* to the container wall. On the other hand, the powder diffraction pattern was obtained for the oblique incident beams. This suggest that the diffractions arose from *randomly* oriented crystal, which were formed inside the colloid due to homogeneous nucleation (**Fig. 3(b)**). The diffraction pattern form the colloidal crystals formed by inhomogeneous and homogeneous nucleation were in consistent with our earlier study by means of the ultra-small-angle x-ray scattering [18]. An influence of μG was found to be less significant for the heterogeneous nucleation process with the aid of the cell walls. Thus, in the following μG experiments we chose the oblique incidence.

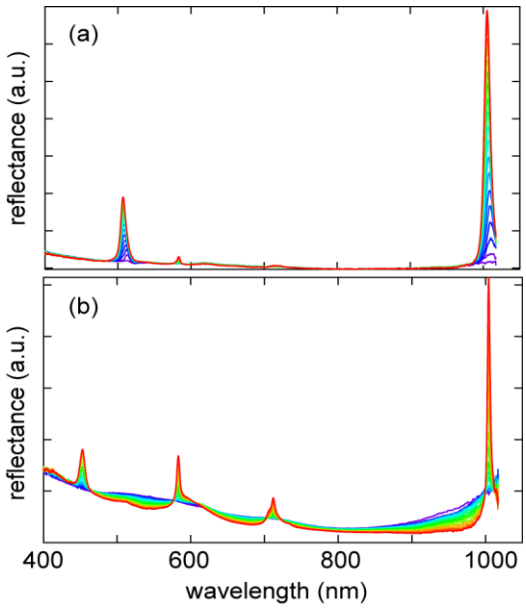

Fig. 6 Reflection spectra of the colloidal crystals under 1G taken by using (a) right angle and (b) oblique angle (approximately 10 degree) incident light beams. Silbol 132.

3.3 Incubation Time of the Crystallization

We examined an influence of μG on the crystallization process from the time evolution of the peak intensity. **Figure 7(a)** and **7(b)** are the reflectivity (reduced by the largest value during the observation) plotted against time t for Silbol 132 (C_p = 2 vol.%) at [NaCl] = 2 μM, and 3 μM, respectively. The curves were averaged ones of at least ten (μG) and three (1G) measurements. The incubation time τ were estimated as inflection points in the reflectivity *vs.* time plots. The τ value at μG and 1G were 3.5 and 2.5 sec at [NaCl] = 3 μM, and 3.0 and 1.5 sec at [NaCl] = 2 μM. That is, τ values became longer under μG environment. τ was somewhat longer at the higher [NaCl], because the electrostatic interaction between the particles is stronger for lower salt concentration, due to the electrostatic screening effect by small ions.

In **Fig. 7(c)**, the data obtained by using right–angle incident beam is shown for comparison (sample: KE-W10, C_p = 4 vol.%; [NaCl] = 4 μM; [NaOH] = 50 μM). τ values at μG and at 1G were not significantly different from each other. This is reasonable, because here we observed the spectra from the crystals grown at the cell walls.

We note that in the growth curve in **Fig. 7(c)** (heterogeneous nucleation), τ value at 1G after the flight experiments was slightly longer than that before the flight. This was presumably due to contamination by a small amount of ionic impurity from sample containers, which reduced the electrostatic interaction magnitude.

On the other hand, in curves in **Figs. 7(a)** and **7(b)** (homogeneous nucleation), τ value at 1G after the flight was shorter than that before. This is explainable if crystallization nuclei were not completely melted by stirring. Even then, the flight experiments gave the largest τ value, which demonstrated a significant μG effect.

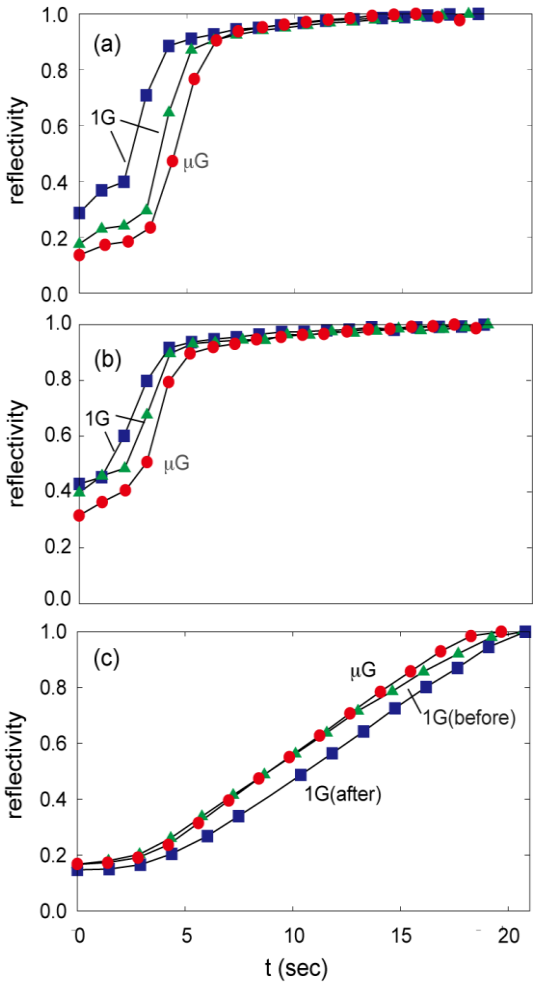

Fig. 7 Time evolution of reflection intensity under 1G (▲;before and ■;after the flight), and ● ;μG (a) Silbol 132, 1.7 vol.%; 2 μM; oblique angle, (b) Silbol 132, 2 vol.%; 3 μM; oblique angle, (c) KE-W10, C_p = 2 vol.%; [NaCl] = 2 μM; right-angle.

3.4 Influence of μG on Diffraction Peak Widths

The width of the Bragg peaks under μG was narrower than that at 1G. **Figure 8** represents the reflection spectra of colloidal crystals (Silbol 132, C_p = 2 vol.%, [NaCl] = 3 μM). Magnified spectra around the first peaks are shown in an inset figure. λ_m value of the first peak lay at around 920 nm. Other peaks were attributable to the diffraction from the higher order BCC lattice planes. The data at 1G before and after the flight were also shown for comparison. The full width at half maximum (FWHM) of the first peak clearly decreased under μG. Generally FWHM value of the diffraction peak, δ, is inversely proportional to the crystal size. According to Scherrer's relation for diffraction peak width[7,19], δ is given by

$$\delta = K\lambda / (D\cos\theta), \tag{3}$$

where K is the constant, D the crystal size, λ and θ are

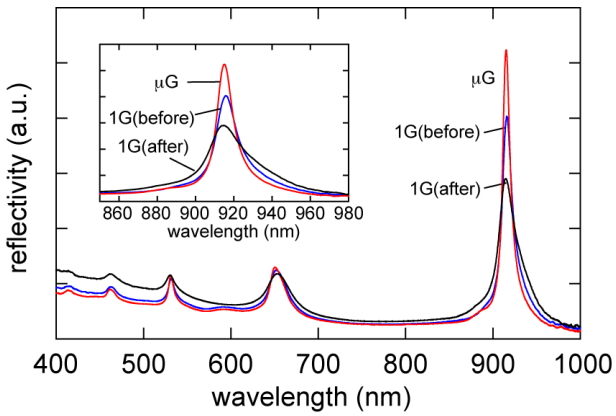

Fig. 8 The reflection spectra under 1G (before and after the flight) and μG. Silbol 132; C_p =1.7 vol.%; [NaCl] = 2 μM; oblique angle. A magnified figure for the first peak is shown in an inset figure.

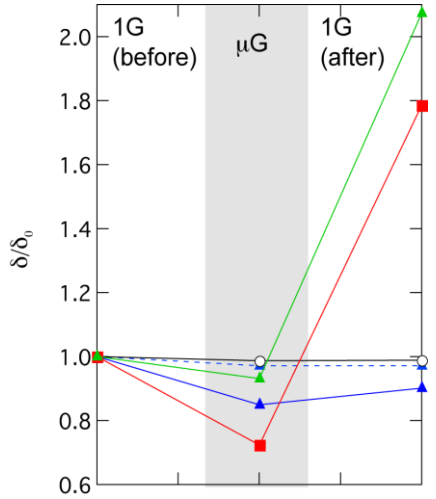

Fig. 9 Variations of the relative FWHM values, δ/δ_0, under 1G (before and after the flight) and μG. Sample; Silbol 132. ○, C_p =2 vol.%; [NaCl] = 1 μM. ▲, C_p =1.7 vol.%; [NaCl] = 2 μM. ▲, C_p = 2 vol.%; [NaCl] = 2 μM (dashed and solid lines are the right- and oblique-angle reflection). ■, C_p = 2 vol.%; [NaCl] = 3 μM.

wavelength and diffraction angle of x-ray. Thus, the larger value of δ observed under μG is explainable, if the size of crystals or crystal grains formed under μG was larger comparing with those at 1G. The smaller value of δ under μG was observed for most of the samples we have examined. **Figure 9** compares the δ value at 1G (before and after the flights) and under μG are compiled (the δ values were reduced by the value at 1G before the flights, δ_0). In **Fig. 9**, reduction of δ/δ_0 during μG condition is clearly seen.

4. Conclusions

In the present paper, we reported the results of spectroscopy study during our aircraft parabolic flight experiments carried out in January and February 2016. An influence of μG was found to be less significant for the heterogeneous nucleation process with the aid of the cell walls. We observed that (i) an incubation time τ of the homogeneous nucleation under μG is larger than that in 1G, and (ii) FWHM of the Bragg peak under μG was narrower than that in 1G. Because the peak width is inversely proportional to crystal size, the finding (ii) suggests that larger crystals were formed under μG. This appears to be due to smaller nucleation rate at μG and should result in longer τ under μG. We have not expected all these observations, and to the best of our knowledge, they have not anticipated theoretically. In order to understand nucleation kinetics of the colloidal crystals, we need to measure incubation time for nucleation as a function of colloid concentration. Further studies are in progress.

Acknowledgments

The aircraft parabolic flight experiments have been performed as a collaboration project “Crystal growth rate from super-cooled states”, by JAXA, Nagoya City University, and Osaka University. We would like to express sincere gratitude to Diamond Air Service Co. Ltd. for their kind help on performing the parabolic flight experiments. Our sincere thanks are due to Mr. Fumio Uchida and Mr. Hiroki Imai of Fuji Chemical Co., Ltd. for their kind donating the Silbol colloidal silica samples.

References

1) P. Pieranski: Contemp. Phys. **24** (1983) 25.
2) W.B. Russel, D.A. Saville and W.R. Schowalter: Colloidal Dispersions, Cambridge University Press, New York (1989).
3) A.K. Sood: Solid State Phys., H.Ehrenreich and D.Turnbull eds., Academic Press, New York (1991).
4) N. Ise and I. Sogami: Structure Formation in Solution, Springer, Berlin (2005).
5) J. Yamanaka, T. Okuzono and A. Toyotama: “Colloidal Crystals", in Pattern Formation, S. Kinoshita ed., Elsevier, Amsterdam (2013).
6) J. Zhu, M. Li, R. Rogers, W. Meyer and R.H. Ottewill: STS-73 Space Shuttle Crew, W.B. Russel and P.M. Chaikin: Nature **387** (1997) 883.
7) M. Ishikawa, H. Morimoto, T. Maekawa and T. Okubo: Int. J. Mod. Phys., **B16** (2002) 338.
8) T. Okubo, A. Tsuchida, T. Okuda, K. Fujitsuna, M. Ishikawa, T. Morita and T. Tada: Colloid Surf., **160** (1999) 311.
9) A. Tsuchida, K. Taguchi, E. Takyo, H. Yoshimi, S. Kiriyama, T. Okubo and M. Ishikawa: Colloid Polym. Sci., **278** (2000) 872.
10) H.J. Shöpe and P. Wette: Phys.Rev.E, **83** (2011) 051405.
11) M.Murai, T.Okuzono, M.Yamamoto, A.Toyotama and J. Yamanaka: J. Colloid Interf. Sci., **370** (2012) 39.
12) A. Toyotama, M. Yamamoto, Y. Nakamura, C. Yamasaki, A. Tobinaga, Y. Ohashi, T. Okuzono, H. Ozaki, F. Uchida and J. Yamanaka: Chem. Mater., **26** (2014) 4057.
13) C. Kakihara, A. Toyotama, T. Okuzono, J. Yamanaka, K. Ito, T. Shinohara, M. Tanigawa and I. Sogami: Int. J. Microgravity Sci. Appl., **32** (2015) 320205.
14) K. Tsukamoto: Int. J. Microgravity Sci. Appl., **29** (2012) 106.
15) T. Okubo, A. Tsuchida, S. Takahashi, K. Taguchi and M. Ishikawa: Colloid Polym. Sci., **278** (2000) 202.
16) B.J. Ackerson and N.A. Clark: Phys. Rev. Lett., **46** (1981) 123.
17) C. Kittel: Introduction to Solid State Physics, Sixth Edition, Weily and Sons, New York (1993).
18) J. Yamanaka, H. Yoshida, T. Koga, N. Ise and T. Hashimoto: Phys. Rev. Lett., **80** (1998) 5806.
19) B.D. Cullity: Elements of X-ray diffraction, Second edition, Addison-Wesley, Boston (1978).